



HAL
open science

FSI investigation on stability of downwind sails with an automatic dynamic trimming

Mathieu Durand, Alban Leroyer, Corentin Lothodé, Frédéric Hauville, Michel Visonneau, Ronan Floch, Laurent Guillaume

► **To cite this version:**

Mathieu Durand, Alban Leroyer, Corentin Lothodé, Frédéric Hauville, Michel Visonneau, et al.. FSI investigation on stability of downwind sails with an automatic dynamic trimming. *Ocean Engineering*, 2014, Innovation in High Performance Sailing Yachts - INNOVSAIL, 90, pp.129-139. 10.1016/j.oceaneng.2014.09.021 . hal-01155431

HAL Id: hal-01155431

<https://hal.science/hal-01155431>

Submitted on 30 Nov 2023

HAL is a multi-disciplinary open access archive for the deposit and dissemination of scientific research documents, whether they are published or not. The documents may come from teaching and research institutions in France or abroad, or from public or private research centers.

L'archive ouverte pluridisciplinaire **HAL**, est destinée au dépôt et à la diffusion de documents scientifiques de niveau recherche, publiés ou non, émanant des établissements d'enseignement et de recherche français ou étrangers, des laboratoires publics ou privés.

FSI investigation on stability of downwind sails with an automatic dynamic trimming

Mathieu Durand^{a,*}, Alban Leroyer^b, Corentin Lothodé^a, Frédéric Hauville^c,
Michel Visonneau^b, Ronan Floch^d, Laurent Guillaume^e

^a K-Epsilon company, 1300 route des crêtes, Sophia-Antipolis, France

^b Centrale Nantes/CNRS, LHEEA, UMR6598, 1 rue de la Noë, 44321, Nantes Cedex 3, France

^c Naval Academy Research Institute – IRENav CC600, 29240 Brest Cedex 9, France

^d Incidences-Sails, rue Alain Colas, 29200 Brest, France

^e BSG-Développements, 2 rue de l'Echelle Chauvin, 17000 La Rochelle, France

Gennakers are lightweight and flexible sails, used for downwind sailing configurations. Qualities sought for this kind of sail are propulsive force and dynamic stability. To simulate accurately the flow surrounding a sail, several problems need to be solved. Firstly, the structural code has to take into account cloth behavior, orientation and reinforcements. Moreover, wrinkles need to be taken into account through modeling or fine enough discretization. Secondly, the fluid solver needs to reproduce the atmospheric boundary layer as an input boundary condition, and be able to simulate separation. Thirdly, the fluid-structure interaction (FSI) is strongly coupled due to the lightness and the flexibility of the structure. The added mass is three orders of magnitude greater than the mass of the sail, and large structural displacement occur, which makes the coupling between the two solvers difficult to achieve. Finally, the problem is unsteady, and dynamic trimming is important to the simulation of gennakers (Graf and Renzsch, 2006). As the FSI procedure is detailed in Durand (2012), the present work is rather focused on its application to downwind sail stability.

The main objective of this paper is to use numerical simulations to model gennakers, in order to predict both propulsive force and sail dynamic stability. Recent developments from Durand (2012) are used to solve these problems mentioned earlier, using a finite element structural analysis program dedicated to sails and rig simulations coupled with an unsteady Reynolds averaged Navier–Stokes equations (URANSE) solver. The FSI coupling is done through a partitioned approach with quasi-monolithic properties. An arbitrary Lagrangian Eulerian (ALE) formulation is used, hence the fluid mesh follows the structural deformation while keeping the same topology. The fluid mesh deformation is carried out with a fast, robust and parallelized method based on the propagation of the deformation state of the sail boundary fluid faces (Durand et al., 2010).

Tests were realized on a complete production chain: a sail designer from Incidences-Sails has designed two different shapes of an IMOCA60 gennaker with the SailPack software. An automatic procedure was developed to transfer data from Sailpack to a structure input file taking into account the orientation of sailcloth and reinforcements. The same automatic procedure is used for both gennakers, in order to compare dynamic stability and propulsion forces. A new method is then developed to quantify the practical stability of a downwind sail.

1. Introduction

1.1. Unsteady FSI on downwind sails

In recent years, CFD computations for sailing yachts and specifically for sails have increased considerably the performance

of yachts sails. Most publications on FSI have concentrated on upwind sails. Downwind sails, due to their lightweight and instabilities are more frequently treated with experimental procedure (Renzsch and Graf, 2011), or with CFD around a rigid structure, see for example Viola (2009). Several publications try to simulate the complex flow and the steady response of the downwind structure (Graf and Renzsch, 2006, Trimarchi, 2012, Lombardi, 2012). Trimarchi et al. (2013) is mainly dedicated to the structure model using shell finite elements capturing the wrinkling behavior without any model, but without real

* Corresponding author. Tel.: +33 4 89 86 69 25.
E-mail address: mathieu@k-epsilon.com (M. Durand).

interaction since a constant pressure loading is used to represent the operating condition of the sail. Several publications try to simulate the complex flow and the steady response of the downwind structure (Graf and Renzsch, 2006, Trimarchi, 2012, Lombardi, 2012). The latter also starts to investigate a transient FSI computation. Recently, Lombardi et al., (2012) and Parolini and Lombardi (2013) show fully coupled FSI computations of a downwind sail modeled without any trimming using a shell finite-element model for the structure and a URANSE solver for the fluid. The use of a shell model results in the introduction of a bending stiffness to the sail, while, in the present work, the sail is modeled with membrane elements without bending stiffness. Furthermore, the coupling is achieved using a classical Dirichlet-Neumann coupling algorithm associated with an Aitken relaxation, which is less efficient than the algorithm presented here.

1.2. Goals of downwind sails

Sail designers use specific software such as Sailpack to define the constructed sail shape, called the molded shape based on their experience to develop a flying shape. Sail designers try to optimize the parameters to maximize the propulsive force, while keeping the most stable flying gennaker.

Stability is essential for gennakers, particularly for single-handed boats. From a practical point of view, stability can be defined by sailmakers as the capability of the sail to maintain its trimmed shape. It has therefore the meaning of flying shape robustness, resistance to collapse, minimal need to dynamic trimming. The leading edge of a trimmed gennaker is very light and has a periodic behavior. When the sail is breaking (i.e. curling) on the luff, a stable gennaker does not need to have the trim adjusted: it is unfolding on its own. In the case of an unstable gennaker, a crew member must adjust the trim or bear away to unfold the gennaker. Unfortunately, this behavior is very sensitive to wind variations and to the boat motions. This phenomenon cannot be quantified by standard stability assessment procedures. The criterion used here comes from the sailor's perspective. Since this notion of stability refers to an unsteady behavior, it is therefore mandatory to develop a dynamic FSI procedure to refine the design analysis through time accurate computational results. This is the reason why a specific trimming procedure has also been developed in this study to mimic as much as possible the mechanism affecting the stability of gennaker. In this study, we investigate two real gennakers built, tested and used during the last Vendée Globe. Thus, the two gennakers are really close in terms of their design, but have different performances. Those differences are small, but significant for both sailors and sailmakers. These two gennakers have been digitized and then compared for one wind condition, taking into account the atmospheric boundary layer.

2. ARA coupled with FINE™/Marine: a complete unsteady tool for FSI sailing applications

Modeling the wind, sail and rig interactions on a sailing yacht is a complex subject, because the quality of the simulation depends on the accuracy of both the structural and fluid simulations, which strongly interact. Moreover, loads on sails are prone to high unsteady oscillations due to waves, wind variations, course changes or trimming for example, but sometimes also due to the unsteadiness of the flow itself (vortex shedding, unsteady separation location, etc.). The problem for downwind sails is even more complex because the flow is often detached from the sails. Furthermore, sails are subject to large deformations which can produce large changes to the flying shape. IRENav, K-Epsilon and

the DSPM group of LHEEA have jointly developed a coupled computational tool able to compute the fluid-structure interaction characterizing the dynamic behavior of sails in wind.

This coupled simulation tool is composed of an original finite element code ARA (Durand, 2012, Augier, 2012) developed by K-Epsilon to model sails and the rig of sailing boats (mast, shrouds, sheets, etc.) in order to predict forces, tensile and shape of sails as a function of loads. This code is coupled to the incompressible turbulent flow solver ISIS-CFD, developed by the DSPM group of LHEEA (Wackers et al., 2011, Leroyer and Visonneau, 2005, Queutey and Visonneau, 2007) and internationally distributed by NUMECA Int. as FINE™/Marine.

2.1. Structural solver

The solver ARA is based on a non-linear finite element formulation derived through the use of the virtual work principle. Each sail panel is modeled using CST (Constant Strain Triangles) membrane elements within the finite strain theory. Large rotations and large strains are then accurately handled. Despite its simplicity (constant stresses, constant strains and uniform stiffness of the material for each element), this choice has proven to give a good ratio of accuracy to computer power. Non-linearities coming from compressions are taken into account. A wrinkle model is also included to accurately resolve the local deformations of sails without having a huge number of elements. It is based on a modification of the stress-strain tensor described in Nakashino and Natori (2005), according to the definition of three states: taut state, where the sail is completely in tension, wrinkled state, where tension is restricted to one direction, and slack state, where the sail is completely in compression. The modification leads to a consistent tangent stiffness matrix where changes in both the wrinkling direction and the amount of wrinkling are taken into account. The sail structure and paneling are imported from the sail designer software SailPack developed by BSG Développements. The latter is used to make the sails and the structural mesh in accordance to the sail design. An anisotropic composite material where several layers may be superimposed is used to model the stress-strain relationship of the sail fabric.

In order to represent a complete sailboat rig (spars, battens, shrouds and running rigging), models of a cable and a 3D beam were implemented too. Specific joints allow the accurate simulation of pulleys, luff of the sails, the forestay, the sail batten gusset and the management of collision.

The temporal discretization is driven by a Newmark-Bossak scheme (Wood et al., 1980) and the resolution is ensured by a Newton method through the computation of the tangent matrix associated with an Aitken relaxation. For more detail, the reader is referred to Durand (2012).

2.2. Fluid solver

ISIS-CFD solves the incompressible URANS equations. It is based on a fully unstructured, finite-volume method to build the spatial discretization of the conservation equations. The flow equations are constructed face by face which means that cells having an arbitrary number of arbitrarily shaped faces can be accepted. The temporal discretization scheme is the implicit 2-step Backward Differentiation Formula (BDF2) scheme when dealing with unsteady configurations. For each time step, an inner loop (denoted as a non-linear loop) associated to a Picard linearization is used to solve the non-linearities of the system. The velocity field is obtained from the momentum conservation equations and the pressure field is extracted from the mass conservation constraint, or continuity equation, transformed into a pressure equation, through a SIMPLE-like method. In the case of turbulent flows,

additional transport equations for modeled variables are solved in a form similar to the momentum equations and they can be discretized and solved using the same principles (Duvigneau and Visonneau, 2003). An Arbitrary Lagrangian Eulerian (ALE) formulation is used to take into account modification of the fluid spatial domain due to body motion and deformation (Leroyer et al., 2008). Free-surface flow is addressed with an interface capturing method, by solving a conservation equation for the volume fraction of water, with specific compressive discretization schemes (Queutey and Visonneau, 2007). The code is fully parallel using the MPI (Message Passing Interface) protocol. An anisotropic automatic grid refinement technique is also included (Wackers et al., 2012).

2.3. Fluid structure algorithm

The fluid-structure interaction between sails and wind is a difficult problem because it is strongly coupled. As stated previously, the added mass on a gennaker is typically three orders of magnitude larger than the mass of the structure. Adding to this difficulty is the fact that the structure has almost no bending stiffness, this makes it a very difficult coupled problem. Such a physical configuration also appears in biological flows as hemodynamics (Quaini, 2009), except that in the latter case internal flows are concerned. When the added mass effect is strong, weakly coupled methodologies classically used in aeroelasticity fail to reach a stable solution due to the fact that a large part of the fluid force depends on the acceleration of the structure (Söding, 2001). However for such a case, even iterative partitioned approaches (also denoted block-iterative approaches) cannot provide a stable coupling within a reasonable CPU time. To achieve a stable and efficient coupling between the two solvers, the structural resolution is therefore integrated within the non-linear loop of the fluid solver, as it was previously done in Hay et al. (2006) and Leroyer and Visonneau (2005), for rigid bodies and bodies with imposed deformation, respectively. This approach is also suggested in Badia and Codina (2007). The non-linear loop becomes the FSI loop when the resolution of the structural part is included (see Fig. 1).

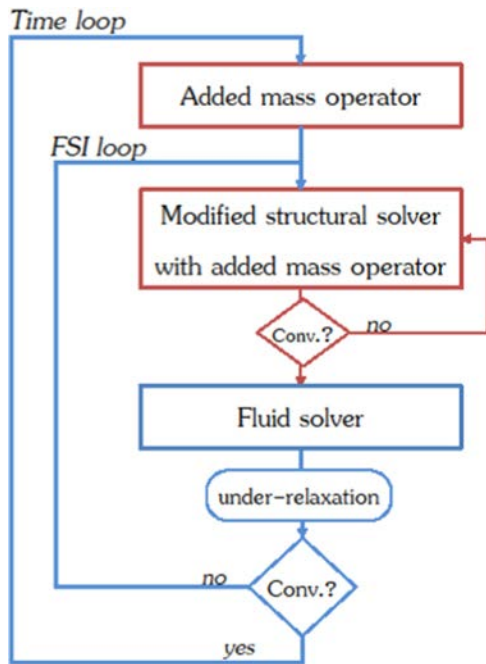


Fig. 1. FSI partitioned algorithm: fluid algorithm in blue coupling with structural solver and additional Jacobian (added mass operator) in red. (For interpretation of the references to color in this figure legend, the reader is referred to the web version of this article.)

The structural solver is also modified to integrate the short-time fluid response which is given by the added mass operator (Badia et al., 2008, Joosten et al., 2009). Here, the latter is approximated with the help of a potential inviscid fluid solver AVANTI based on panel method and vortex particle method from Rehbach (1977). It is developed by K-Epsilon, and already coupled with the ARA solver. When computing the added mass operator, a second approximation can be made without compromising the efficiency of the coupling: it is diagonalized. Physically, it is equivalent to compute the pressure response from a unit normal acceleration on each sail. The operator is then added in the structural equations (see Eq.(5)).

Although not monolithic, this algorithm is very stable, fast and parallelized. The number of FSI iterations to converge a time step is similar to the number of non-linear iterations for an unsteady fluid configuration without FSI. Indeed, it can be viewed as an approximated (and then iterative) block-LU factorization of the monolithic system.

Let us represent the linearized monolithic system as Eq.(1).

$$\begin{bmatrix} F & C_{sf} \\ C_{fs} & S \end{bmatrix} \begin{Bmatrix} x_f \\ x_s \end{Bmatrix} = \begin{Bmatrix} s_f \\ s_s \end{Bmatrix} \quad (1)$$

where F and S refer to the linearized fluid and structure operator, respectively. x_f and x_s represent the fluid and structure variables. The source term of both solvers are denoted by s_f and s_s , for the fluid and structure domain, respectively. C_{fs} and C_{sf} refer to the coupling operator fluid to structure and structure to fluid, respectively. A block-LU factorization of this monolithic system leads to Eq.(2).

$$\begin{cases} (S - C_{fs}F^{-1}C_{sf})x_s = s_s - C_{fs}F^{-1}s_f \\ Fx_f = s_f - C_{sf}x_s \end{cases} \quad (2)$$

By approximating the Jacobian operator of $C_{fs}F^{-1}C_{sf}$ by the opposite of the added mass operator $-Ma$ (Eq.(3)), it can be shown that the monolithic problem can be substituted by the iterative resolution of Eq.(4).

$$(C_{fs}F^{-1}C_{sf})x_s^{k+1} \cong (C_{fs}F^{-1}C_{sf})x_s^k - Ma(x_s^{k+1} - x_s^k) \quad (3)$$

$$\begin{cases} (S + Ma)x_s^{k+1} = s_s - C_{fs}x_f^k + Max_s^k \\ Fx_f^{k+1} = s_f - C_{sf}x_s^{k+1} \end{cases} \quad (4)$$

The first equation of this system Eq.(4) can be rewritten using the Jacobian of the structure matrix J_s under the form of Eq.(5).

$$(J_s + Ma)\delta x_s^{k+1} = -r_s^k - C_{fs}\delta x_f^k \quad (5)$$

where $r_s^k = Sx_s^k + C_{fs}x_f^{k-1} - s_s^k$ means the residual of the structure problem, and $\delta x_s^{k+1} = x_s^{k+1} - x_s^k$ represents the increment of the structure variables between two iterations (same definition for the fluid variable $\delta x_f^k = x_f^k - x_f^{k-1}$).

As a consequence, the block-LU factorization leads to the two steps of the proposed iterative algorithm, namely: a resolution of a modified structure problem and a resolution of the linearized fluid problem (i.e. one iteration of the non-linear loop).

2.4. Load transfer

The load transfer is carried out through an intersection method similar to what is described in section 2.2.2 of De Boer et al., (2007). The computation of all the sub-elements, which is the largest CPU time consuming task of this procedure, only needs to be done once at the beginning of the simulation. Each time it is needed, the fluid load on each element is computed and then distributed to each nodal degree of freedom by minimizing the

deformation energy which makes the nodal transfer unique. An accurate load conservation at the interface is then obtained. Furthermore, an *a posteriori* test is added to check that the difference between the discrete transferred energies on each side (fluid and structure) is negligible with respect to the kinetic energy of the sail. In this work, the sail considered in the fluid mesh had a small thickness (thickness / chord $\approx 2 \times 10^{-6}$), since the mesh generation around bodies without thickness was not available. To solve this problem, fluid nodes are linked to interface elements using a parameterization. These interface elements are built using the normal vectors to the surface structure (see Fig. 2). The parameterization is then conserved during the whole computation and used to deduce the fluid node displacement when the mesh deformation procedure is applied. Other techniques of interpolation such as those described recently in Lombardi et al. (2013) can be used to address the inter-grid interpolation with a better energy conservation transferred at the interface, but this has not yet been implemented in the present work.

2.5. Mesh deformation

A new mesh deformation tool was also developed in Durand (2012) to transmit the deformation of the sails to the fluid domain without having to rebuild a new grid from scratch, thus avoiding interpolation procedures (Fig. 3). This method is based on the combination of an explicit advancing front method and smoothing. It is also parallelized, fast, robust and able to compute the large deformations of an unstructured mesh around multiple bodies like a gennaker and main sail interacting together. The explicit advancing front is based on a computation of the rigid rotation and displacement of each interface element. This rigid motion is then propagated from cell layer to cell layer to the boundaries of the fluid domain. This method is fast, but needs a smoothing algorithm to take into account some cells far from the interface, where the propagation method is not well adapted. In some cases, a cell can be influenced by two different fronts of propagation with different deformations resulting in an unacceptable cell. This is why an explicit smoothing step based on a weighting neighbor deformation is carried out to improve robustness and quality of the mesh.

2.6. Validations

The code's accuracy was validated by an experimental comparison performed on a well-controlled test case with an original experiment developed by IRENav (Durand, 2012, Augier et al.,

2012), which consists of a square of gennaker fabric mounted on two carbon battens which were moved in a forced oscillation (see Fig. 4). In these validations, shape, profile, and motions of the battens (Fig. 5) were measured and compared. Finally, an

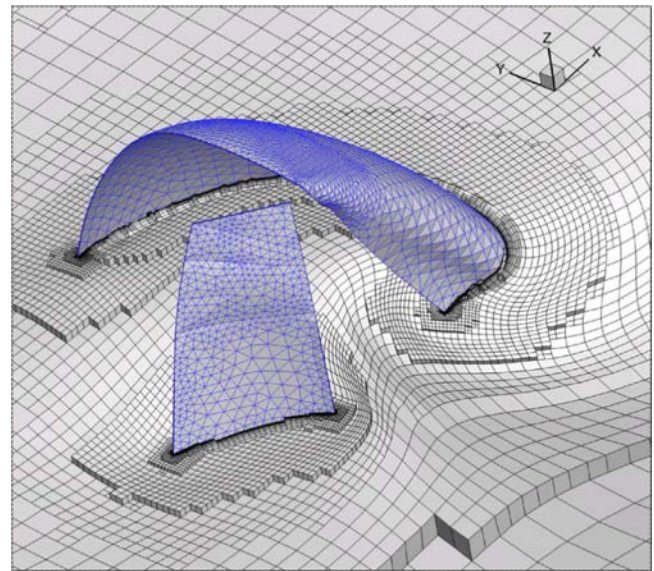


Fig. 3. In black: fluid mesh deformation around a main sail and gennaker, during an unsteady simulation. In blue: structural meshes are displayed. (For interpretation of the references to color in this figure legend, the reader is referred to the web version of this article.)

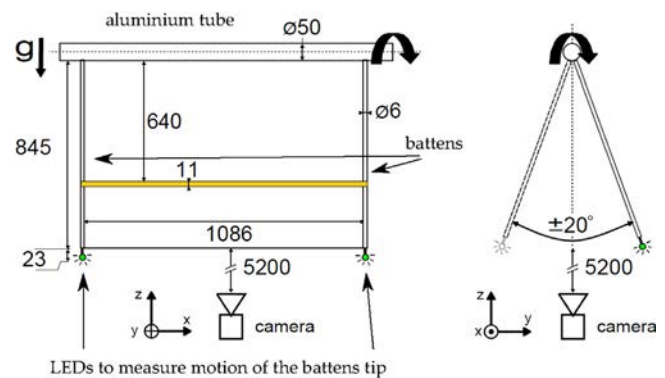


Fig. 4. Scheme of the experiment

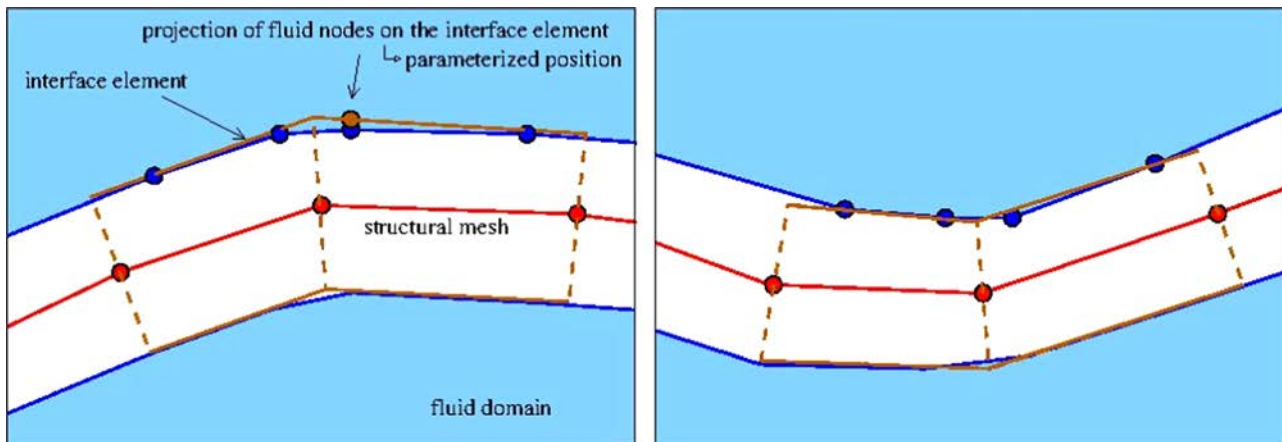


Fig. 2. On left: mesh projection, on right: mesh deformation

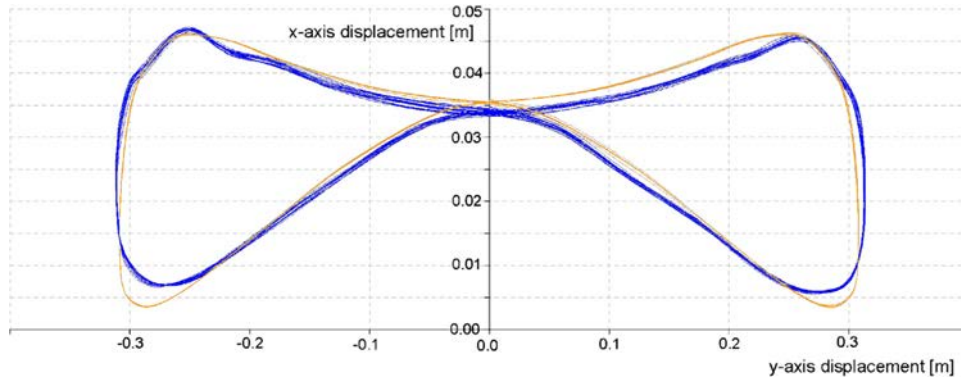


Fig. 5. Comparisons between experiment (blue) and computation (orange) of the behavior of the batten tip. (For interpretation of the references to color in this figure legend, the reader is referred to the web version of this article.)

application was made on an unsteady sailing gennaker with an automatic trimming algorithm, interacting with a mainsail which was realized to illustrate the potential of the present fluid-structure coupling, see Fig. 3 for an example, from Durand (2012). Note that in sections 4, 5 and 6, the main sail was not taken into account.

3. Choice and design of the two gennakers

3.1. Choice

In general, the shapes of gennakers are widely differing, depending on the kind of boat, the range of wind and their use. In this paper, two very similar gennakers are compared, in order to estimate the capability of the process to distinguish the characteristics of closely related sails. These sails were designed and used during the Vendée Globe 2012-2013 by two skippers.

3.2. Design

Once Gennaker A was designed, Gennaker B was a small evolution with the following differences:

- the luff twist is 1% smaller and the luff roach is 0.4% smaller,
- the sail is 1% less twisted,
- the maximum sail camber is 0.7% deeper, and 1% further forward.

The sail areas are identical and the tack, head and clew points are in the same position for both gennakers (Fig. 6).

3.3. Full scale tests

The two sails were tested by sailmakers during full-size sessions in real conditions. During tests, and without measurement, sailors felt that propulsive forces of the two gennakers were close. The goal of the modifications made on the second gennaker was to get more stability. In fact, during test session, the luff of gennaker A was sometimes curling hard, and collapsing. The crew therefore had to modify the trim or bear away. This means that they changed drastically the heading of the boat, in order to increase the incidence on the sail. These modifications of the trim or boat heading decreased the performance of the boat.

The luff of gennaker B had a different behavior: The luff curled moderately, and most of the time, no actions were needed to uncurl the luff.

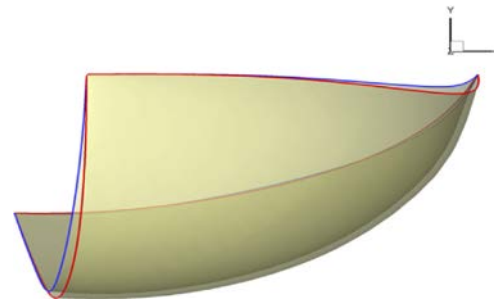


Fig. 6. Top view of the two gennakers as molded: Gennaker A in red, and gennaker B in blue. On the top is the luff (leading edge), on the left is the leech (trailing edge). (For interpretation of the references to color in this figure legend, the reader is referred to the web version of this article.)

4. Gennakers digitalization

Sails were firstly designed by another sailmaker software from the company Incidences-Sails. The real sails were therefore digitized again, using the software Sailpack, in order to respect the initial shape of the mold and to be read as input data for the ARA solver.

The design process is as follows:

- Design of the sail mold in 3D,
- Definition of seam layouts,
- Definition of patch layouts,
- Definition of the cloth properties, the doubled or tripled layers and the orientation of the cloth for each panel.

From this information, SailPack calculated the 2D panels that were used to build the real sail. Then a triangular mesh is generated for each 2D panel. The outline nodes of the meshes were connected to simulate the assembly of the sail. All the nodes were then moved to recompose the sail in 3D, keeping the 2D initial node distances. In this way the resulting 3D mesh is based on the 2D panels that are used for the real assembly of the sail.

Stiffness matrices were associated to each mesh element. The cloth, its orientation and the number of layers were taken into account. The Fig. 7 shows the stiffness of the cloth, defined as an invariant of the stiffness tensor (C_{ij}) :

$$\sqrt{C_{11}^2 + C_{11}C_{12} + C_{12}^2 + C_{12}C_{22} + C_{22}^2 - C_{11}C_{22} + 3C_{13}^2 + 6C_{23}C_{13} + 3C_{23}^2}.$$

Additional reinforcements were made with not deformable patches of 20 cm radius around the three points. The structural model was composed of about 7000 membrane elements, with one cable element for the sheet. The stiffness matrices of each

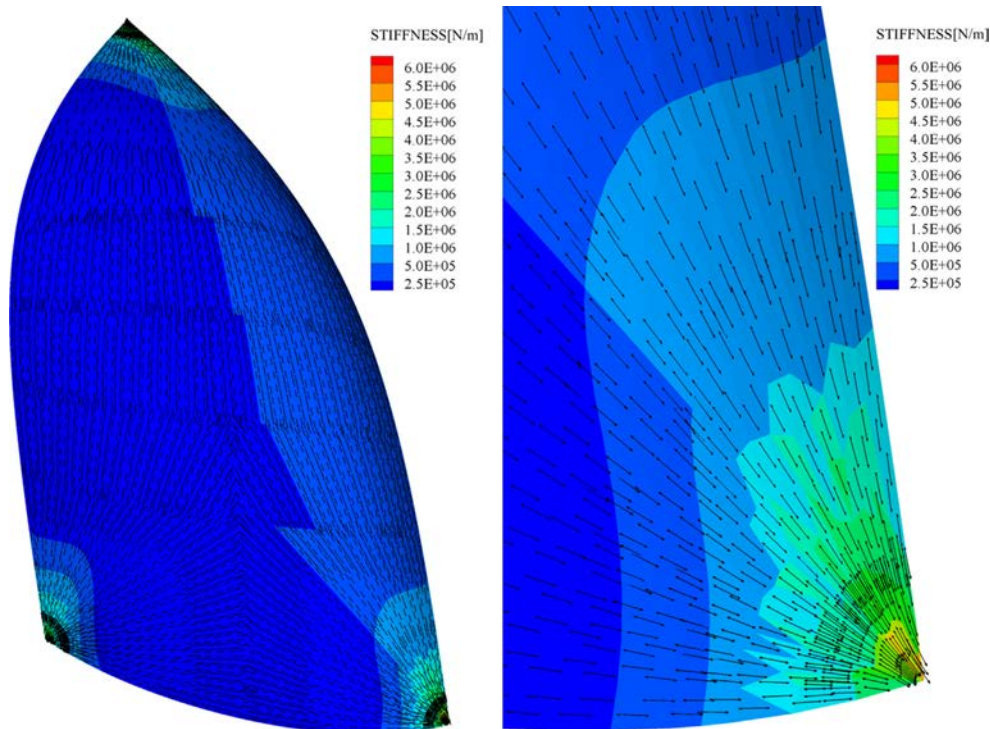


Fig. 7. Left: View of the stiffness of the gennaker. Right: zoom on the tack point. Arrays symbolize the direction of maximal stiffness.

material used were provided from tests on each cloth pieces. To simplify the computation, the mainsail and all rigging were not meshed, and were not simulated.

5. Simulation process

The steps of a computation can be summarized as follows:

- Structural computation with uniform pressure,
- Fluid meshing of the resulting shape,
- Fluid computation to initialize the flow field,
- Unsteady FSI with trimming procedure.

This procedure aims to limit the deformation of the mesh and then to keep an adequate mesh quality during the unsteady FSI computation.

5.1. Structural computation

In the first step, a structural computation is made with a uniform pressure difference on the sail. The length of the sheet is modified in order to roughly orientate the sail correctly according to the incoming flow. This first step gives the shape of the sail which is used to generate the initial volume fluid mesh after.

5.2. Fluid meshing

In the second step, the meshing around the deformed sail is done through HexpressTM, a fully hexahedral, automated mesh generator based on the octree method. The wind direction crosses the computational domain diagonally. The two inlet external boundaries are located at about 120m from the sail, whereas a larger distance of 240m is chosen for the two outlet external boundaries to recover a quite undisturbed flow, when leaving the

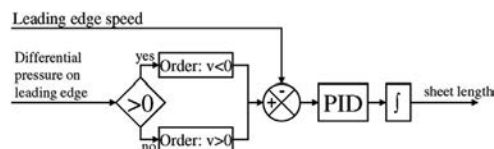


Fig. 8. The trimming algorithm.

fluid domain. The domain is set to 120 m height. The bottom of this domain ($z=0$) represents the sea level.

Cells are refined along the z -axis over the whole height of the domain to take into account the presence of the atmospheric boundary layer, with finer cells close to $z=0$ where the velocity gradient is higher. Refinement was also carried out near the sail. The entire model is meshed with 1.8 million cells. Fluid boundary condition on the sail is set as a wall function with a Y^+ value of 30. Based on the knowledge previously learned on the validation cases, such a mesh looks fine enough for RANS computations around a single sail with a wall function approach to have the discretization error under control. Even if it would be nice to show it again on this configuration, no mesh refinement study was performed in this work.

5.3. Fluid computation

An initial fluid computation is required before starting an unsteady FSI simulation. Conditions on boundaries are implemented to simulate the atmospheric boundary layer. A boat speed of 5.92 m/s is used in conjunction with a logarithmic boundary layer ($Z_0=0.002$ m); true wind speed measured at 30 m is 7.72 m/s, true wind angle is 150 degrees. The apparent wind speed at $z=15$ m is about 2.6 m/s. The time for an air particle to travel from the luff to the leech was 3.5 s at $z=15$ m.

5.4. Unsteady FSI

The wind turbulence as gusts of the incident flow due to the atmospheric turbulence is a phenomenon which can also be

significant but far more difficult to take into account into a numerical simulation. It would induce complex unsteady inlet boundary conditions and the definition of a spectrum depending on the weather conditions, hard to model and to control. To reach

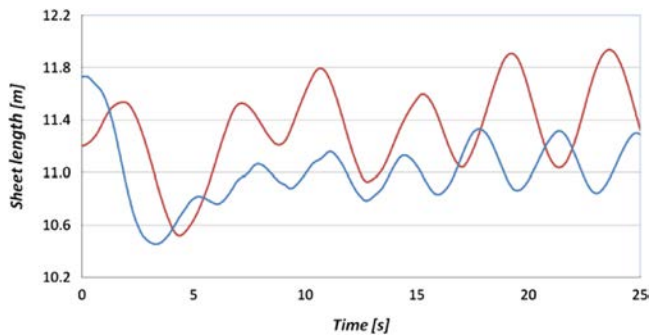


Fig. 9. Result of trimming algorithm on the length of the two gennakers sheets (red line: gen. A, blue line: gen. B): variations showing the instability of the gennakers. (For interpretation of the references to color in this figure legend, the reader is referred to the web version of this article.)

a meaningful statistics of the response, the CPU time would certainly be multiplied by at least a factor of 100, as it is the case when we want to deal with a spectrum of irregular waves in hydrodynamics. Moreover, a LES or at least a DES approach would be for sure more appropriate to accurately propagate this specific boundary condition. A finer mesh would then be required. This is up to now beyond the capacities of both modeling and computer power. The boat is also supposed to have no secondary motion, even if it would be easier to impose compared to the previous issue.

The computations were performed on 2 dual-processor hexacore Xeon X5670 (24 cores) and took 3 days each. The FSI coupling procedure was started from the converged structure and converged fluid of the initial configuration. All the computations were performed with unsteady RANSE, using the k-omega SST turbulence model (Menter, 1994). The simulation time was performed over 25 seconds for each case. Such a long time was necessary to obtain periodic results.

The computation time is divided into about 15 % for the structure solver and 85 % for the fluid solver. Inside the fluid

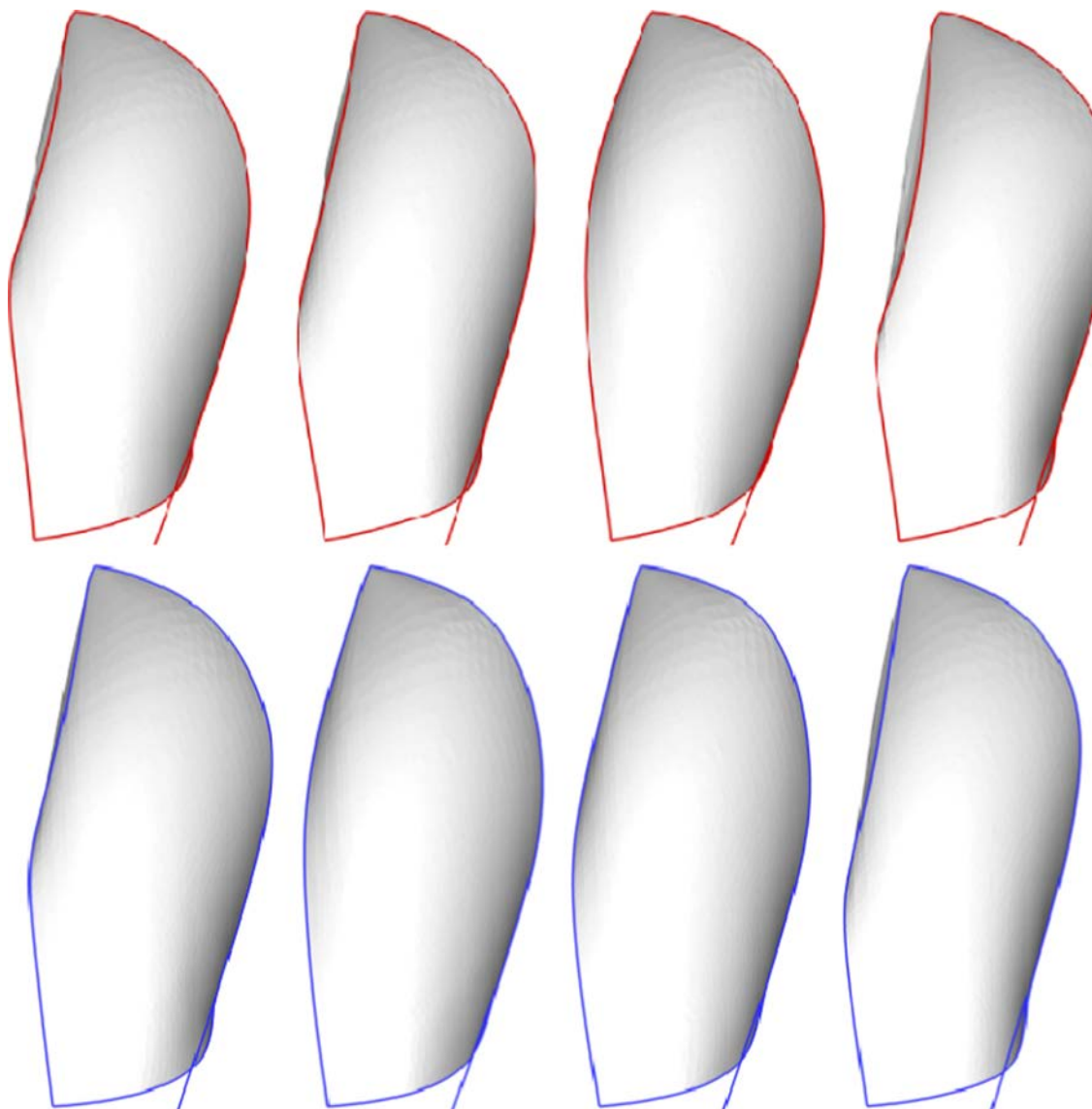


Fig. 10. Comparison of the behavior of the luff for the two gennakers during 4 steps of the period. Shade with lightning effects. Gennaker A on the top, gennaker B on the bottom.

solver, the mesh deformation procedure costs about 10 % of the CPU time for this case.

5.5. Trimming procedure

The trimming algorithm (Fig. 8) is defined in order to reach the objective of zero pressure difference between each side close to the leading edge. This algorithm measures this differential pressure on the leading edge, and gives a trimming order such that the leading edge normal velocity is in opposition with the direction of the pressure force. The value of the desired velocity is set as a parameter, and depends on the size of the sail. Then a signal treatment with the leading edge velocity measurement is carried out: a PID treatment is made on the error between the measured and target values. This value is the velocity command of the gennaker sheet. This command is then integrated to obtain the sheet length. This procedure is dynamic: the length of the sheet is therefore always changing.

Some tests were needed to adjust the PID parameters. Too violent of a trimming algorithm works like a “pumping” trimmer, some waves appear and propagate on the sail. With too slow of an algorithm, the luff collapses hard, and the computation could stop, due to the limits of the mesh deformations.

6. Results and comparisons between the two gennakers

Fig. 9 shows the result of the trimming algorithm for both gennakers. During the first five seconds, the large amplitude is related to the bad trim position of the gennaker at the start (see Section 5). Then after a transition period, the length of the sheet slowly becomes periodic, and after 17 s of simulation it has become fully periodic. During periodic motion, the luff begins curling; the sail leading edge velocity is in the direction of folding the luff further. Then the algorithm pulls on the sheet. The algorithm does not wait for uncurling: when the velocity of the leading edge is inverted, the algorithm stops pull on and begins to ease the sheet. The consequence on the leading edge is a periodic curling and uncurling behavior.

The curling phenomenon is known to be used as a main visual mark by the professional skippers. Computations performed on gennakers have shown that curling occurrence corresponds to a velocity field which remains attached to the sail with the maximum of length, whereas the cases without curling lead to detached flows from the leading edge.

The initial stage of curling is difficult to analyze here, since we start from a configuration which does not correspond to an equilibrium between fluid and structure. As explained in section 5, the structure shape comes from an initialization with uniform pressure as fluid loads, resulting in quite a realistic shape and the initial flow is given by a first computation without FSI coupling around this shape. As a consequence, we have preferred to focus on the asymptotic periodic behavior. The behavior of both gennakers controlled by the automatic trimming algorithm is periodic, and very similar to the behavior of real life gennakers. Four snapshots of the gennaker shape are shown in Fig. 10 during one period of the asymptotic behavior. The curling phenomenon is characterized by the successive folding and unfolding of the sail luff. It is noticeable that the curling amplitude (Fig. 10) and the sheet length variation (Fig. 9) are higher for gennaker A than for gennaker B. Moreover, the oscillation period is longer for gennaker A ($Tp=4.4$ s) than for gennaker B ($Tp=3.5$ s).

Other results, reported Fig. 11, Fig. 12 and Fig. 13, come from an averaging procedure over the last two periods of the motion. Positions, as well as pressure and elongation have been averaged. Fig. 11 shows the mean flying shape of both gennakers. Even if only the sail's luff is different in the design shapes, the average luff position in both flying shapes are very similar, as the flying luff position is mainly controlled by the oncoming flow. However, significant differences are observed in both flying shapes in the middle and rear areas: for gennaker B, the twist is reduced and the clew is moved rearward (shorter sheet length). We think that it is worthwhile to underline that, thanks to the FSI procedure, it is possible to predict a global shape modification of a sail implied by a very local change of the geometry. Fig. 12 shows the differential pressure between pressure and suction faces of the sail. The trimming algorithm tries to obtain a zero pressure difference on the leading edge, this is accomplished for half of the luff: the upper

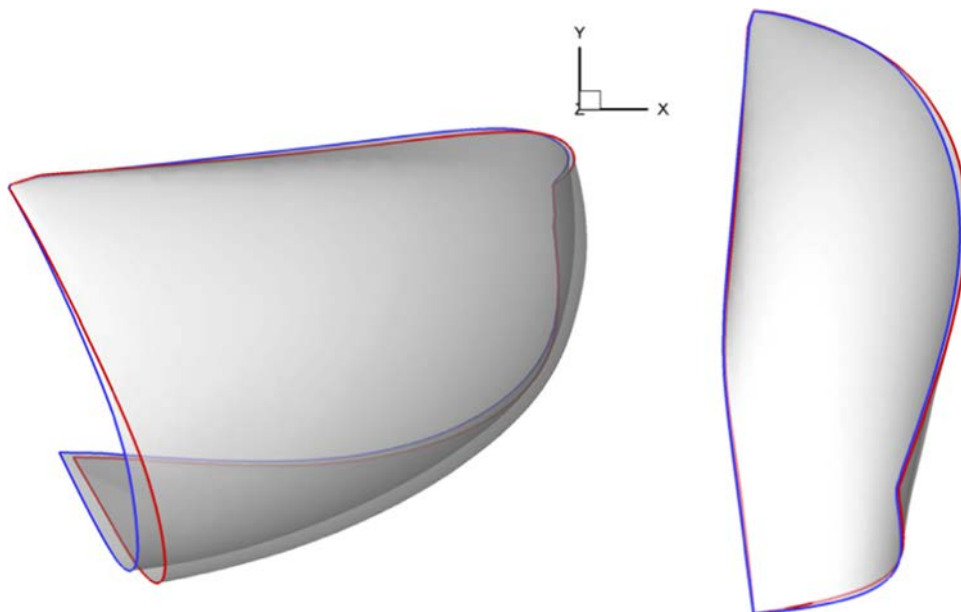


Fig. 11. Top and aft views of the averaged flying shape during computation: Gennaker A in Red, and Gennaker B in blue. (For interpretation of the references to color in this figure legend, the reader is referred to the web version of this article.)

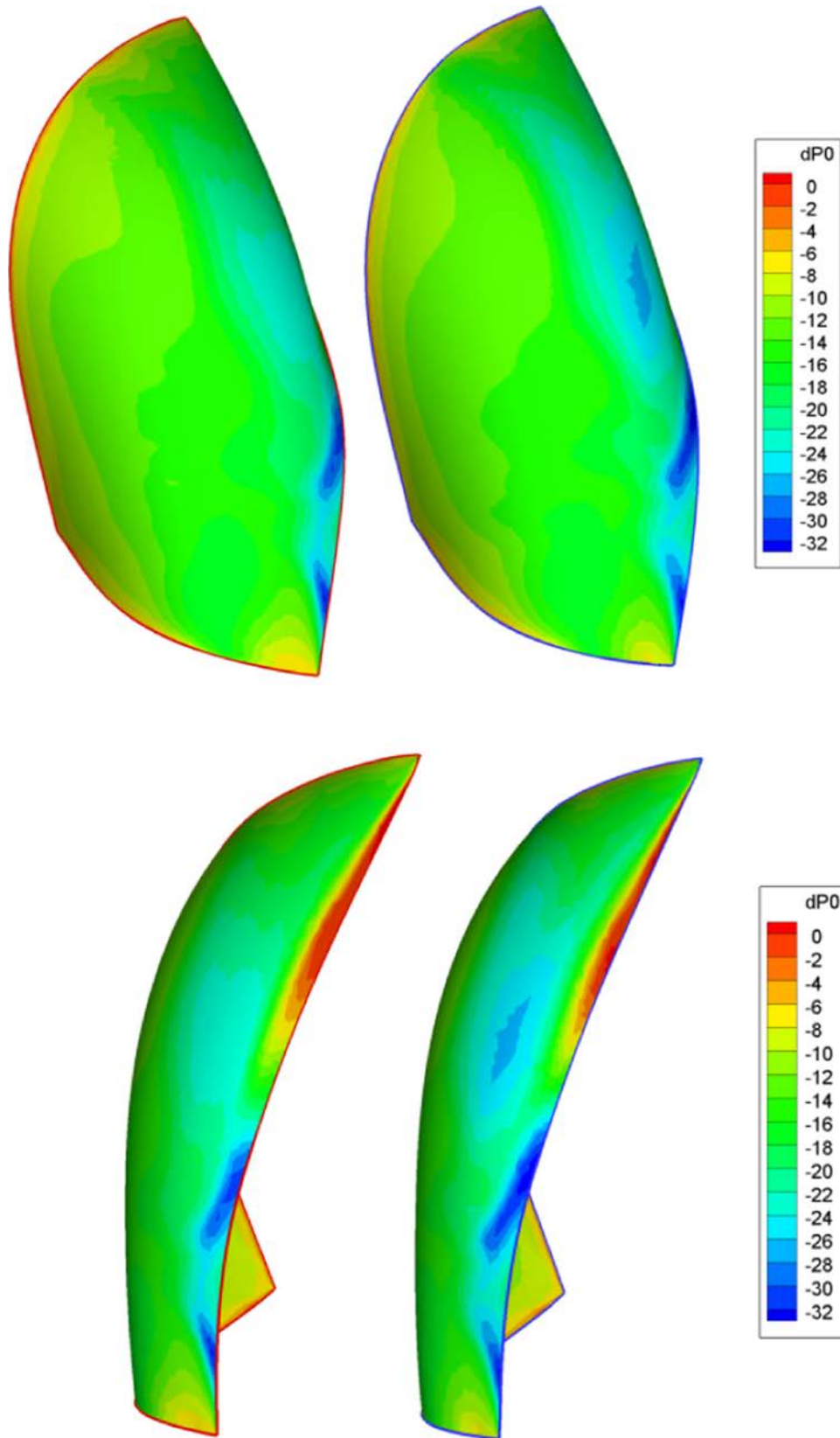


Fig. 12. Two views of the averaged differential pressure (pressure–suction, [Pa]) during two periods: gennaker A on the left, gennaker B on the right.

half has a mean pressure difference close to zero. This is indicative of an attached flow on this part of the sail. In the lower part, where the luff is not curling, the negative pressure difference on the leading edge indicates a detached flow. Global pressure values are

quite similar between the two sails, but gennaker B has a larger pressure difference.

From these results, we propose an adimensional parameter of the stability denoted by S , dependent on the trimming algorithm,

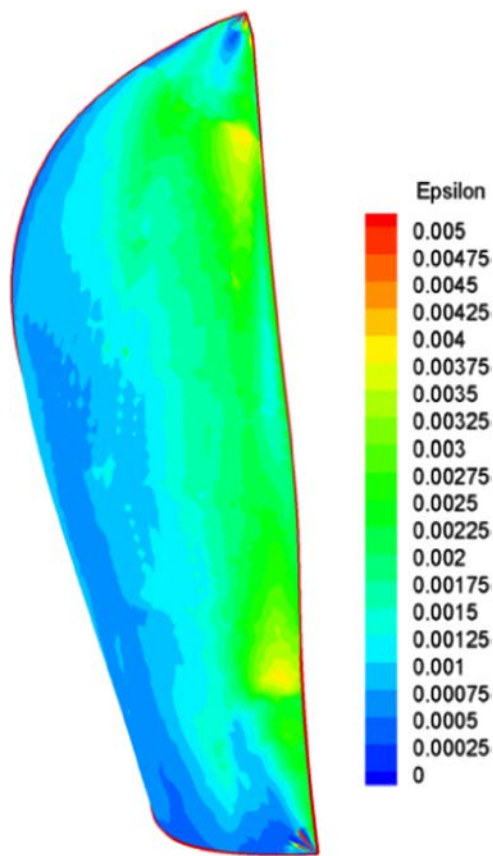


Fig. 13. Front view of averaged strain on gennaker A. Yellow represents 0.4% of strain in the cloth. (For interpretation of the references to color in this figure legend, the reader is referred to the web version of this article.)

Table 1
Summary of the differences measured between the two gennakers.

	<i>Gennaker A</i>	<i>Gennaker B</i>	<i>Difference (%)</i>
Propulsive force [N]	3625	3737	+3.1
Side force [N]	1555	1684	+8.3
Vertical force [N]	1223	1335	+9.2
Stability parameter S	34	64	+85

based on the height of the sail H divided by the amplitude of the trimming A :

$$S = H/A$$

The term stability is used here from a practical point of view while sailing, with the meaning of flying shape robustness, resistance to collapse, minimal need to dynamic trimming or over-sheeting.

Even if the trimming procedure does not reproduce the action of a skipper in operation, this automatic trimming of the gennaker sheet length can give information about the behavior of the sail. If a sail is more prone to oscillate with this procedure, we can assume that this sail, initially correctly trimmed, will be more reactive to a perturbation and then will be more prone to collapse. Since the trimming procedure is identical for the two tested sails, a small amplitude of the trimming indicates a sail which could support larger perturbations without collapsing. In that sense, the parameter S can give information about the stability of the sail: the lower the amplitude of oscillations is, the more stable the sail can be considered, and the higher the parameter S is.

A summary of time-averaged global results is given in Table 1: gennaker B results in a gain of 85% in *stability* and more than 3%

higher drive force compared to gennaker A. However, the side force is also increased by 8.3%, which is detrimental to sailing performance. The detailed analysis of performance gain or loss would need to run a VPP to assess the sailing performance in both cases, but the impact of stability would be difficult to account for, even with a state-of-the-art dynamic VPP. In the context of this paper, it can be stated that gennaker B is significantly more stable than gennaker A and is likely to result in a higher boat speed, particularly if the maximum righting moment is not reached. Sailmakers are also interested in other results such as the deformation of the cloth: Fig. 13 shows the mean strain in the cloth. This is the average during two periods of the norm of the strain. Maximum deformation of about 0.4% occurs near the luff, on both sides, near the reinforcements.

7. Conclusion

In this work, unsteady fluid-structure interaction on downwind sails is investigated. These computations are based on the coupling between two advanced models for both fluid and structure: a URANSE fluid solver using an ALE approach to deal with flexible bodies and a FE sail-oriented solver able to take into account the rigs of the boats, the reinforcements of the sail and including a wrinkle model.

The key points of the codes coupling are described to achieve a stable and efficient approach, despite of very strong added mass effects. Associated to an automatic trimming procedure implemented into this numerical tool, it is shown that the latter is able to predict the flying shape, as well as the sail forces and the unsteady behavior of gennakers. Then, a complete automatic procedure for the comparison of two real gennakers is described. Despite some simplifying assumptions, especially regarding the wind inlet conditions which is supposed to be steady, the simulation results show very realistic behavior for downwind sails with a periodic curling on the leading edge associated with an oscillation of the sheet length trimming the sail. A quantitative characterization of the sail stability from a sailor's point of view has been presented and gennaker B has been shown to be more stable with regards to this criteria, which may have a great effect on the yacht performance.

One of the goals of this work is to show the ability of this original coupled model to resolve the dynamic FSI behavior of downwind sails and more importantly to reproduce the effects of very small differences in the structure design which may have a great impact on the fluid-structure system's dynamic behavior. In the case of interest here, the behavior differences between both sails were clearly noticed by the sailors in practice, but very challenging to resolve in simulations.

Further investigations with this tool will be carried out, such as the use of hybrid-LES turbulence model, investigation of the influence of the mainsail in terms of the gennaker design and flying shapes. More realistic procedures will be tested with the help of sailmakers and professional sailors. Finally, comparisons will be performed with instrumented gennakers.

References

- Augier, B., 2012. Experimental Studies of the Fluid Structure Interaction on Soft Surfaces: Application to Yacht Sails (Ph.D. Thesis). French Naval Academy Research Institute—IRENav, France.
- Augier, B., Bot, P., Hauville, F., Durand, M., 2012. Experimental validation of unsteady models for fluid structure interaction: application to yacht sails and rigs. *J. Wind Eng. Ind. Aerodyn.* 101, 53–66.
- Badia, S., Codina, R., 2007. On some fluid-structure iterative algorithms using pressure segregation methods. Application to aeroelasticity. *Int. J. Numer. Methods Eng.* 72, 46–71.

- Badia, S., Quaini, A., Quarteroni, A., 2008. Modular vs. non-modular preconditioners for fluid–structure with large added-mass effect. *Comput. Methods Appl. Mech. Eng.* 197, 4216–4232.
- De Boer, A., van Zuijlen, A.H., Bijl, H., 2007. Review of coupling methods for non-matching meshes. *Comput. Methods Appl. Mech. Eng.* 196, 1515–1525.
- Durand, M., 2012. Interaction fluide-structure souple et légère, applications aux voiliers (Ph.D. Thesis). Ecole Centrale Nantes, France.
- Durand, M., Hauville, F., Bot, P., Augier, B., Roux, Y., Leroyer, A., Visonneau, M., 2010. Unsteady numerical simulations of downwind sails. In *Proceedings of the Second International Conference on Innovation in High Performance Sailing Yachts. INNOV/SAIL 2010*, pp. 57–64.
- Duvigneau, R., Visonneau, M., 2003. On the role played by turbulence closures in hull shape optimization at model and full scale. *J. Mar. Sci. Technol.* 8, 11–25.
- Graf, K., Rensch, H., 2006. RANSE investigations of downwind sails and integration into sailing yacht design processes. In *Proceedings of the 2nd High Performance Yacht Design Conference Auckland, 14–16 February*.
- Hay, A., Leroyer, A., Visonneau, M., 2006. H-adaptive Navier-Stokes simulations of free-surface flows around moving bodies. *J. Mar. Sci. Technol.* 11, 1–18.
- Joosten, M., Dettmer, W., Peric, D., 2009. Analysis of the block Gauss–Seidel solution procedure for a strongly coupled model problem with reference to fluid–structure interaction. *Int. J. Numer. Methods Eng.* 78, 757–778.
- Leroyer, A., Visonneau, M., 2005. Methods for RANSE simulations of a self-propelled fish-like body. *J. Fluids Struct.* 20, 975–991.
- Leroyer, A., Barré, S., Kobus, J.M., Visonneau, M., 2008. Experimental and numerical investigations of the flow around an oar blade. *J. Mar. Sci. Technol.* 13, 1–15.
- Lombardi, M., 2012. Numerical simulation of a sailing boat: free surface, fluid-structure interaction and shape optimization (Ph.D. Thesis). Ecole Polytechnique Fédérale de Lausanne, Switzerland.
- Lombardi, M., Cremonesi, M., Giampieri, A., Parolini, N., Quarteroni, A., 2012. A strongly coupled fluid-structure interaction model for wind-sail simulation. In: *Proceedings of the 4th High Performance Yacht Design Conference. The Royal Institution of Naval Architects, London, UK*.
- Lombardi, M., Parolini, N., Quarteroni, A., 2013. Radial basis functions for inter-grid interpolation and mesh motion in FSI problems. *Comput. Methods Appl. Mech. Eng.* 256, 117–131.
- Menter, F., 1994. Two-equation eddy-viscosity turbulence models for engineering applications. *AIAA J.* 32, 1598–1605.
- Nakashino, K., Natori, M.C., 2005. Efficient modification scheme of stress–strain tensor for wrinkled membranes. *AIAA J.* 43 (1), 206–215.
- Parolini, N., Lombardi, M., 2013. Unsteady FSI simulations of downwind sails. In B. Brinkmann and P. Wriggers (Eds), *Proceedings of the V International Conference on Computational Methods in Marine Engineering, MARINE 2013*.
- Quaini, A., 2009. Algorithms for Fluid-Structure Interaction Problems Arising in Hemodynamics (Ph.D. Thesis). Ecole polytechnique fédérale de Lausanne, Switzerland.
- Queutey, P., Visonneau, M., 2007. An interface capturing method for free-surface hydrodynamic flows. *Comput. Fluids* 36, 1481–1510.
- Rehbach, C., 1977. Calcul numérique d'écoulements tri-dimensionnels instationnaires avec nappes tourbillonnaires. *La recherche aérospatiale* 5, 289–298.
- Rensch, H., Graf, K., 2011. An experimental validation case for fluid-structure-interaction simulations of downwind sails. In: *Proceedings of the 21th Chesapeake Sailing Yacht Symposium*.
- Söding, H., 2001. How to integrate free motions of solids in fluids. In: *Proceedings of the 4th Numerical Towing Tank, Symposium, Hamburg*.
- Trimarchi, D., 2012. Analysis of Downwind Sail Structures using Non-Linear Shell Finite Elements (Ph.D. Thesis). University of Southampton, U.K.
- Trimarchi, D., Vidrascu, M., Taunton, D., Turnock, S.R., Chapelle, D., 2013. Wrinkle development analysis in thin sail-like structures using MITC shell finite elements. *Finite Elem. Anal. Des* 64 (2013), 48–64.
- Viola, I., 2009. Downwind sail aerodynamics: a CFD investigation with high grid resolution. *Ocean Eng.* 36, 974–984.
- Wackers, J., Koren, B., Raven, H., Ploeg, A., Starke, A., Deng, G., Queutey, P., Visonneau, M., Hino, T., Ohashi, K., 2011. Free-surface viscous flow solution methods for ship hydrodynamics. *Arch. Comput. Methods Eng.* 18, 1–41.
- Wackers, J., Deng, G., Leroyer, A., Queutey, P., Visonneau, M., 2012. Adaptive grid refinement for hydrodynamic flows. *Comput. Fluids*, 85–100.
- Wood, W., Bossak, M., Zienkiewicz, O.C., 1980. An alpha modification of Newmark's method. *Int. J. Numer. Methods Eng.* 15, 1562–1566.